Quantifying the Driving Effect of Colored Noise in Brownian Motors

Zhichao Zhang[1], Yue Liu[1], Congmin Wu[2*], and Dahai He[1*]

[1]*Department of Physics and Jiujiang Research Institute, Xiamen University, Xiamen 361005, China*
[2]*School of Mathematical Sciences, Xiamen University, Xiamen 361005, China*

(Received 25 October 2024; accepted manuscript online 17 December 2024)

The colored noise disrupts the detailed balance, enabling directed transport in ratchet systems without additional driving forces. Despite a well-established understanding of the conditions for Brownian motors, quantification of the driving effect of colored noise and its connection to deviations from equilibrium remains unexplored. In this study, we examined the directed motion of an overdamped Brownian motor within an asymmetric traveling potential subjected to Ornstein–Uhlenbeck colored noise. We propose a scheme to quantify the driving effect of colored noise by defining an effective force based on the stopping velocity of the traveling potential where directed transport halts. Our results revealed a nonmonotonic dependence of the effective force on the noise correlation time and a monotonic dependence on the noise strength, corresponding to double and single current reversals, respectively. The nonmonotonicity of the current is attributed to the interplay between the fluctuating characteristics and the driving effects of colored noise.

DOI: 10.1088/0256-307X/42/1/014401 CSTR: 32039.14.0256-307X.42.1.014401

1. Introduction. Brownian motors have attracted considerable attention for decades owing to their ability to rectify fluctuating forces into directional motions.[1–3] Breaking symmetry and being in a nonequilibrium state are essential conditions for achieving directed transport.[4] This insight laid the groundwork for the development of various types of Brownian motors such as the rocking ratchet,[5] flashing ratchet,[6,7] and correlation ratchet,[8,9] each of which introduces unbiased mechanisms that break the detailed balance to drive the system out of equilibrium. These studies reveal a rich set of phenomena, including stochastic resonance,[10] multiple current reversals,[11] and absolute negative mobility (ANM).[12] Beyond their theoretical interest, the mechanisms of Brownian motors are highly relevant to biological systems and synthetic applications. Their ability to generate directed transport without external driving forces provides a foundation for understanding and controlling processes, such as intracellular transport,[13,14] muscle contraction,[15] and the separation of microscopic particles.[16,17]

In earlier Brownian motion studies, noise was typically modeled as zero-mean δ-correlated Gaussian-distributed white noise. Although this idealization is convenient, it is unrealistic, because producing such noise requires infinite power. In real-world systems and experimental settings, the correlation time of stochastic forces is usually comparable to or even exceeds the characteristic time of the system.[18] This leads to colored noise with a nonuniform power spectrum. Ornstein–Uhlenbeck (OU) noise is one of the most commonly used types of noise and is characterized by an exponentially decaying time-correlation function. Ratchet systems driven solely by colored noise, known as correlation ratchets, have attracted wide interest because of their ability to generate directed transport under unbiased noise alone. In recent years, active matter research has attracted renewed attention to colored noise. It is often used to describe the self-propelling forces of active particles, thereby forming a bridge between the study of active matter and Brownian motors.[19–23] Models such as the active Ornstein-Uhlenbeck particle share similar mathematical structures with correlation ratchets driven by OU noise.[24,25] The disruption of the detailed balance by the external colored noise stems from its violation of the fluctuation dissipation theorem, which requires the damping and fluctuation forces to be linked by memory friction.[26] Recent studies have advanced our understanding of how colored noise contributes to irreversibility[27] and deviations from equilibrium.[28] Despite extensive studies on Brownian motors with colored noise, the quantification of the driving effect of colored noise, particularly the relationship between the ratchet effect and the degree of deviation from equilibrium, remains elusive.

In this study, we attempt to address this problem by studying the Langevin dynamics of an overdamped Brownian motor subjected to an asymmetric traveling potential and Ornstein–Uhlenbeck noise. We observed a current reversal controlled by the parameters of the colored noise occurring in the direction of the traveling potential. We provide a measurement of the effective force, defined by the stopping velocity of the traveling potential, to quantify the driving effect of colored noise. In addition, we investigated the distinct roles of the correlation between time and noise strength.

The remainder of this paper is organized as follows. In

*Corresponding author. Email: cmwu@xmu.edu.cn; dhe@xmu.edu.cn
© 2025 Chinese Physical Society and IOP Publishing Ltd. All rights, including for text and data mining, AI training, and similar technologies, are reserved.

Section 2, details of the studied Brownian motor model and the colored noise used are introduced. In Section 3, the numerical results are discussed. Finally, a summary is presented in Section 4.

2. Model and Method. In this study, we consider an overdamped Brownian particle subjected to external colored noise through a traveling ratchet potential. The dynamics of the particles are given by Langevin's equation

$$\gamma\dot{x} = -V'(x,\, t) + \xi(t), \tag{1}$$

where x is the position coordinate and γ is the viscous coefficient. Here, $\xi(t)$ is the OU noise with zero mean $\langle\xi(t)\rangle = 0$ and an exponentially decayed time-correlation function $\langle\xi(t)\xi(t')\rangle = \frac{Q}{\tau}\exp(-\frac{1}{\tau}|t-t'|)$, where τ represents the noise correlation time and Q is the overall noise strength. This Gaussian colored noise can be generated using the following Langevin equation:

$$\dot{\xi} = -\frac{1}{\tau}\xi + \frac{\sqrt{2Q}}{\tau}\eta(t), \tag{2}$$

where $\eta(t)$ is Gaussian white noise that satisfies $\langle\eta(t)\rangle = 0$ and $\langle\eta(t)\eta(t')\rangle = \delta(t-t')$.

We consider the traveling ratchet potential [29]

$$V(x,\, t) = V_0(x - ut), \tag{3}$$

where

$$V_0(x) = \frac{U}{2\pi}\Big(\sin\frac{2\pi x}{L} + \frac{1}{4}\sin\frac{4\pi x}{L}\Big), \tag{4}$$

where u denotes the wave velocity, L denotes spatial periodicity, and $\frac{U}{2\pi}$ denotes the potential height. By the transform $y(t) = x(t) - ut$, we can rewrite the dynamic equation as

$$\gamma\dot{y} = -\gamma u - V_0'(y) + \xi(t), \tag{5}$$

which is also referred to as a tilted ratchet [30] with a tilting force $f \equiv -\gamma u$.

For simplicity, we introduce the characteristic length L, characteristic energy of the landscape U, and characteristic time of the system $t_{\rm s} \equiv \frac{\gamma L^2}{U}$. We then obtain a dimensionless form of the above equations:

$$\begin{aligned}
\dot{\tilde{x}} &= \dot{\tilde{y}} + \tilde{u},\\
\dot{\tilde{y}} &= -\tilde{u} - \tilde{V}_0'(\tilde{y}) + \tilde{\xi}(\tilde{t}),\\
\dot{\tilde{\xi}} &= \frac{1}{\tilde{\tau}}\Big[-\tilde{\xi} + \sqrt{2\tilde{Q}}\tilde{\eta}(\tilde{t})\Big],
\end{aligned} \tag{6}$$

and

$$\tilde{V}_0(\chi) = \frac{1}{2\pi}\Big(\sin 2\pi\chi + \frac{1}{4}\sin 4\pi\chi\Big). \tag{7}$$

The dimensionless parameters were rescaled as $\tilde{x} = x/L$, $\tilde{y} = y/L$, $\tilde{t} = t/t_{\rm s}$, $\tilde{V} = V/U$, $\tilde{u} = (t_{\rm s}/L)u$, $\tilde{\xi} = (L/U)\xi$, $\tilde{Q} = Q/(\gamma U)$, $\tilde{\eta}(\tilde{t}) = \sqrt{t_{\rm s}}\eta(t)$, and $\tilde{\tau} = \tau/t_{\rm s}$. If not emphasized, we omit all tilde symbols in the following text.

For nonequilibrium periodic systems, we are most interested in the asymptotic current J, which is given by

$$J \equiv \langle\dot{x}\rangle = \lim_{t\to\infty}\frac{x(t) - x(0)}{t}, \tag{8}$$

The net current extracted from the colored noise by the ratchet potential is defined as

$$J_{\rm c} \equiv J|_{u=0}. \tag{9}$$

Although the non-Markovian characteristics and time dependence of the potential in Eq. (6) is removed, the corresponding two-dimensional Fokker–Planck equation remains analytically intractable. The existing approximation methods perform poorly for intermediate noise-correlation times. We employed the second-order stochastic Runge–Kutta method to numerically solve the Langevin equations (6). To ensure the validity of our simulations, we carefully checked the algorithm and simulation parameters. The integration time step was set to 0.001, which is at least 50 times smaller than the correlation time of noise, to ensure correct statistical distribution. The initial 10^8 time steps were ignored and a steady current was obtained over 10^9 time steps.

3. Results and Discussion. To understand the dynamics of a colored noise-driven Brownian motor in a traveling potential environment, we present numerical results showing the dependence of the current J on the velocity u of the traveling potential for both the adiabatic ($Q = 0$) and non-adiabatic cases ($Q \neq 0$), as shown in Fig. 1. In the adiabatic case or for white noise, there is no current for $u = 0$ because the system is in an equilibrium state and the current always follows the direction of the traveling potential. Notably, for a larger u, a negative differential mobility behavior was observed. In the adiabatic case, the linear region for small u corresponds to a locked state for which the particle is "trapped" since the drifting force γu is too small to allow the particle to escape the potential well. Thus, the particles move along with the traveling potential passively. When u becomes sufficiently large or noise is introduced, the driving force overwhelms the trapping force from the potential, and the system enters a running state with a decrease in the current. At a large u limit, the particle became stationary relative to the traveling potential, which acted as a rapidly oscillating periodic force. Consequently, for a very large u, the current vanishes as the system averages the fast oscillations.

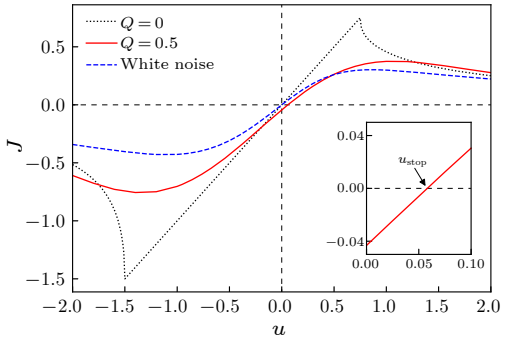

Fig. 1. The current J as a function of the wave velocity u. $Q = 0$ is the adiabatic case without noise. $Q = 0.5$ corresponds to the colored noise case with correlation time $\tau = 1$. In the white noise case, the colored noise is replaced by the white noise of dimensionless strength $k_{\rm B}T/U = 0.1$. The inset highlights the details of the colored noise case. The arrow denotes the definition of $u_{\rm stop}$ (see text for details).

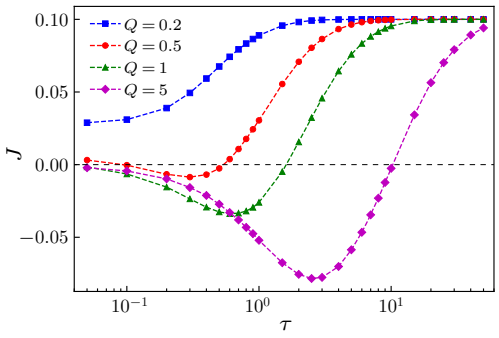

Fig. 2. The current J as a function of noise correlation time τ for different noise strengths Q, with the wave velocity $u = 0.1$.

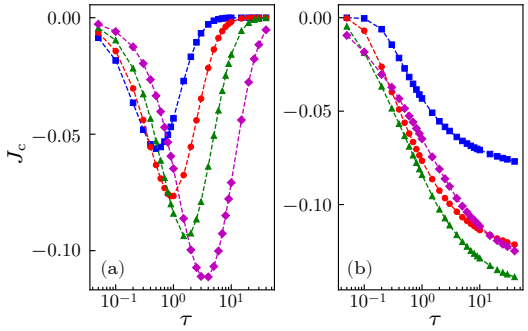

Fig. 3. The net current J_c induced by the colored noise as a function of τ for different values of (a) noise strength Q and (b) noise magnitude (variance) $\langle\xi^2\rangle = Q/\tau$. In plots (a), J_c is given for $Q = 0.5$ (squares), $Q = 1$ (circles), $Q = 2$ (triangles), and $Q = 5$ (diamond). In plots (b), J_c is given for $Q/\tau = 0.5$ (squares), $Q/\tau = 1$ (circles), $Q/\tau = 2$ (triangles), and $Q/\tau = 5$ (diamond).

When external colored noise exists, the current at $u = 0$ is no longer zero, because colored noise disrupts the detailed balance of the system. At low u, when the direction is opposite to the ratchet's "forward" motion, colored noise can drive the Brownian motor against the wave direction until the traveling potential dominates, causing current reversal. The critical point, where the current is zero, reflects the balance between the thermodynamic force induced by the rectified colored noise in the ratchet and the opposing effective force exerted by the traveling potential. The corresponding stopping velocity is denoted as $u_{\rm stop}$ (see the inset in Fig. 1), with the effective force of the rectified colored noise is given by

$$F_{\rm eff} = -\gamma u_{\rm stop}. \tag{10}$$

In our dimensionless formulation, the parameter γ is omitted. In what follows, we first study the directed motion driven by colored noise and then provide a quantitative understanding via the effective force.

The effect of the correlation time τ on the colored noise is shown in Fig. 2 for a wave velocity of $u = 0.1$. As τ increases, the current shifts in the negative direction, which corresponds to the forward direction of the ratchet potential. For a low noise strength Q, the system is dominated by the traveling potential, resulting in consistent motion in one direction. At larger Q (e.g., $Q = 0.5$ in Fig. 2), a double-current reversal is observed, suggesting that the driving effect of colored noise surpasses that of the traveling potential in the intermediate τ regime. For even higher Q, the first current reversal occurs at much lower τ values; however, this region is not contained because of the requirement for significantly smaller integration time steps.

At a small τ limit, the noise approaches the white-noise regime, where no net current is generated in the absence of a deterministic drive, as expected at equilibrium. White noise disrupts directed transport, resulting in a much smaller current compared with the adiabatic case. As τ increases, the system moves further from equilibrium, enhancing the driving effect of colored noise. However, for a fixed noise strength Q, the noise magnitude $\langle\xi^2\rangle = Q/\tau$ decreases as τ increases. Consequently, both J in Fig. 2 and J_c in Fig. 3(a) exhibit nonmonotonic responses to τ, reflecting an antagonism between the system's deviation from equilibrium and the diminishing noise magnitude. Eventually, because the noise vanishes at $\tau \to \infty$, the current depends solely on u. By contrast, Fig. 3(b) shows that for a fixed noise magnitude (variance), the net current J_c increases monotonically with τ, suggesting a positive correlation between the degree of deviation from equilibrium and the driving effect of colored noise. Similarly, for a small u, J exhibits a monotonic dependence on τ.

Next, we present the relationship between J and Q in Fig. 4. Under the condition $u = 0.1$, as Q increases, we initially observe the current monotonically shifting in the negative direction, followed by a current reversal, eventually reaching its maximum intensity (or maximum negative current). Afterward, the current decreases, approaching zero asymptotically from one side. This nonmonotonic behavior arises because of the competition between the fluctuations that hinder directed transport and the driving effect of colored noise. As the intensity of the colored noise increased, the system moved further away from equilibrium, consequently enhancing the noise-driven current. However, as the noise intensity further increases, the fluctuations become sufficiently large to reduce the effective asymmetry of the system, which is essential for the rectification effect and leads to a decrease in the noise-driven current. Additionally, the fluctuations have a monotonic weakening effect on the traveling wave drive, reducing the coupling between the traveling wave and particle. For a large Q limit, both driving effects are diminished, and the current approaches zero.

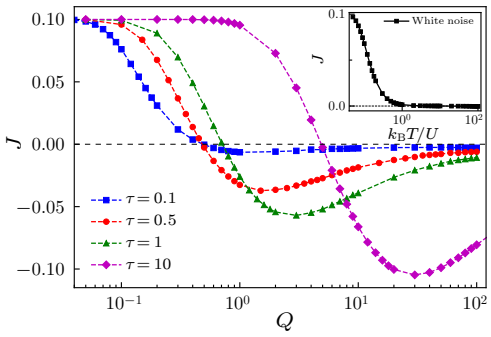

Fig. 4. The current J as a function of noise strength Q for different noise correlation time τ, with the wave velocity $u = 0.1$. The inset shows the case for white noise, where $k_{\rm B}T/U$ is the dimensionless noise strength.

To quantify the driving effect of colored noise in the ratchet system, we measured the effective force F_{eff} using Eq. (10), as shown in Fig. 5. When τ varies with a fixed noise strength Q, F_{eff} follows a bell-shaped curve that initially increases and then decreases as τ increases. This nonmonotonic behavior arises from the tradeoff between the system's departure from equilibrium and the decreasing noise magnitude $\langle \xi^2 \rangle = Q/\tau$. By contrast, when Q/τ is held constant, F_{eff} increases monotonically with τ, as shown in the inset of Fig. 5. Both patterns align with the trend of J_c shown in Figs. 3(a) and 3(b). Additionally, Fig. 5 reveals a monotonic increase in F_{eff} with Q, in contrast to the nonmonotonic response of J to Q in Fig. 4. This suggests that as the fluctuations increase, the driving effect of the traveling wave decays faster than the rectification effect of the colored noise, making it increasingly difficult for the traveling wave to counteract noise-induced driving. Consequently, a second current reversal did not occur, as shown in Fig. 4. Moreover, the fluctuating nature of colored noise indicates a weaker "mobility" at higher noise magnitudes. For the same F_{eff}, a smaller noise magnitude results in a higher J_c, which explains the shift in the peak of J_c in Fig. 3(a) relative to the peak of F_{eff} in Fig. 5.

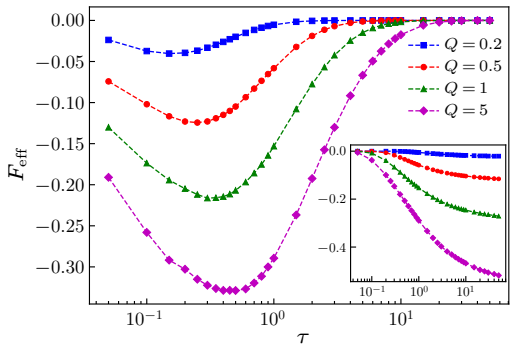

Fig. 5. The effective force of colored noise, as defined in Eq. (10), is plotted as a function of τ for $Q = 0.2$, 0.5, 1, and 2. The inset shows the behaviors when $Q/\tau = 0.2$ (squares), 0.5 (circles), 1 (triangles), and 2 (diamond).

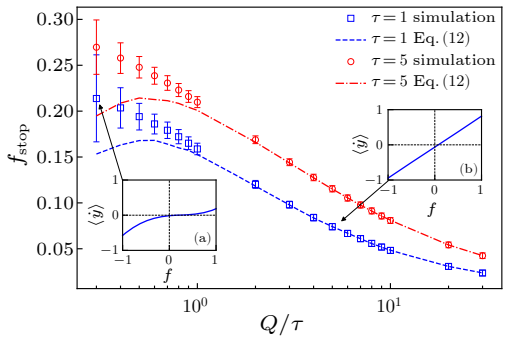

Fig. 6. The stopping force as a function of noise variance for the tilted ratchet. The markers represent the direct measurement for the condition of $\langle \dot{y} \rangle = 0$ by numerical simulations, while the lines represent the estimated stopping force by Eq. (12). The error bars indicate the range for $|\langle \dot{y} \rangle(f)| < \epsilon$. Here, we set $\epsilon = 0.003$, which represents the precision of our numerical simulations. Inset: the current $\langle \dot{y} \rangle$ as a function of external force f for (a) $Q/\tau = 0.3$ and (b) $Q/\tau = 5$, both with $\tau = 1$.

For comparison, we considered the tilted ratchet system given by Eq. (5), where the stopping force f_{stop} is defined as the external force f that stalls the current.[8] In the linear response regime, where the mobility $\mu \equiv \partial \langle \dot{y} \rangle / \partial f$ is approximately constant, the current in the tilted ratchet is given by

$$\langle \dot{y} \rangle = \mu (f - f_{\text{stop}}). \tag{11}$$

In the weak driving regime, where u is small, the current response to the traveling velocity can be approximated as: $J \approx (1 - \gamma\mu)(u - u_{\text{stop}})$. This leads to the following estimate of f_{stop}

$$-\frac{\gamma}{f_{\text{stop}}} = \frac{1}{u_{\text{stop}}} + \frac{1}{J_c}. \tag{12}$$

A comparison between the direct measurement of f_{stop} and the estimation using Eq. (12) is shown in Fig. 6. The two approaches agree well in the regime of large Q/τ, where the $\langle \dot{y} \rangle - f$ curve is closely linear [inset (b)]. Nevertheless, their deviations increase as Q/τ decreases, for which the $\langle \dot{y} \rangle - f$ curve is nonlinear [inset (a)]. In practice, measuring f_{stop} becomes extremely difficult in the case of a small Q/τ, because the slope of the $\langle \dot{y} \rangle - f$ curve decreases [inset (a)]. For the adiabatic case, f_{stop} corresponds to the region in which f cannot induce a flow. Note that f_{stop} and J_c disappear when Q/τ approaches zero. Thus, as shown in Fig. 6, Eq. (12) provides physically reasonable results in the weak-noise regime.

4. Summary. In summary, we studied the directed transport of a Brownian motor driven by colored noise and a periodic asymmetric traveling potential. Our investigation revealed nonmonotonic current behavior and current reversals in response to variations in the noise parameters. In particular, we propose a definition of effective force to quantify the driving effect of colored noise. We found that the effective force increases monotonically with noise strength but exhibits a nonmonotonic dependence on the correlation time. This nonmonotonicity results from the tradeoff between the disruption of the detailed balance and the diminishing noise magnitude as the correlation time increases. Consequently, tuning the correlation time enables up to two current reversals, whereas adjusting the noise strength allows at most one reversal. Furthermore, the response of the current to the effective force is nonlinear because of the interplay between the fluctuating nature and the driving effect of colored noise. In addition, a comparison with the stopping force in the tilted ratchet system demonstrated the advantages of using the stopping velocity in the traveling-wave system to measure the effective force, particularly when the noise magnitude was small.

Notably, the concept of effective force is well defined and relevant in our simple overdamped one-dimensional setup, in which ANM is absent. However, ANM exists in overdamped Brownian motion with a complex topology,[31] collective effects,[32] and underdamped systems.[12] Nevertheless, the role and physical interpretation of the effective force when ANM is present requires further investigation.

Acknowledgment. This work was supported by the National Natural Science Foundation of China (Grant

Nos. 12075199 and 12247172), the Natural Science Foundation of Fujian Province, China (Grant No. 2021J01006), and the Natural Science Foundation of Jiangxi Province, China (Grant No. 20212BAB201024). Numerical simulations were performed on TianHe-1 (A) at the National Supercomputer Center in Tianjin.

References

[1] Hänggi P and Marchesoni F 2009 *Rev. Mod. Phys.* **81** 387
[2] Reimann P 2002 *Phys. Rep.* **361** 57
[3] Zheng Z and Gang H 2016 *From Dynamics to Statistical Physics* (Peking University Publishing House, Beijing)
[4] Feynman R P, Leighton R B, and Sands M *1963 The Feynman Lectures on Physics* **1** (Addison-Wesley)
[5] Schwemmer C, Fringes S, Duerig U, Ryu Y K, and Knoll A W 2018 *Phys. Rev. Lett.* **121** 104102
[6] Reimann P 1997 *Phys. Rep.* **290** 149
[7] Bao J D and Zhuo Y Z 1998 *Phys. Lett. A* **239** 228
[8] Bartussek R, Reimann P, and Hänggi P 1996 *Phys. Rev. Lett.* **76** 1166
[9] Peskin C S, Ermentrout G B, and Oster G F 1994 *Cell Mechanics and Cellular Engineering* (Springer, New York, NY) p. 479
[10] Gammaitoni L, Hänggi P, Jung P, and Marchesoni F 1998 *Rev. Mod. Phys.* **70** 223
[11] de Souza Silva C C, Van de Vondel J, Morelle M, and Moshchalkov V V 2006 *Nature* **440** 651
[12] Machura L, Kostur M, Talkner P, Łuczka J, and Hänggi P 2007 *Phys. Rev. Lett.* **98** 040601
[13] Bressloff P C and Newby J M 2013 *Rev. Mod. Phys.* **85** 135
[14] Vale R D and Milligan R A 2000 *Science* **288** 88
[15] Kull F J and Endow S A 2013 *J. Cell Sci.* **126** 9
[16] Ou G, Stuurman N, D'Ambrosio M, and Vale R D 2010 *Science* **330** 677
[17] Słapik A, Łuczka J, Hänggi P, and Spiechowicz J 2019 *Phys. Rev. Lett.* **122** 070602
[18] Häunggi P and Jung P 1994 *Adv. Chem. Phys.* **89** 239
[19] Ghosh P K, Misko V R, Marchesoni F, and Nori F 2013 *Phys. Rev. Lett.* **110** 268301
[20] Koumakis N, Maggi C, and Leonardo R D 2014 *Soft Matter* **10** 5695
[21] Reichhardt C J O and Reichhardt C 2017 *Annu. Rev. Condens. Matter Phys.* **8** 51
[22] Maes C 2020 *Phys. Rev. Lett.* **125** 208001
[23] Zhou Y, Li Y, and Marchesoni F 2023 *Chin. Phys. Lett.* **40** 100505
[24] Bonilla L L 2019 *Phys. Rev. E* **100** 022601
[25] Muhsin M and Sahoo M 2023 *Phys. Rev. E* **107** 054601
[26] Zwanzig R 2001 *Nonequilibrium Statistical Mechanics* (Oxford University Press)
[27] Gradziuk G, Torregrosa G, and Broedersz C P 2022 *Phys. Rev. E* **105** 024118
[28] Fodor É, Nardini C, Cates M E, Tailleur J, Visco P, and van Wijland F 2016 *Phys. Rev. Lett.* **117** 038103
[29] Borromeo M and Marchesoni F 1998 *Phys. Lett. A* **249** 199
[30] Risken H 1996 *The Fokker–Planck Equation: Methods of Solution and Applications* **18** (Springer, Berlin, Heidelberg)
[31] Eichhorn R, Reimann P, and Hänggi P 2002 *Phys. Rev. Lett.* **88** 190601
[32] Januszewski M and Łuczka J 2011 *Phys. Rev. E* **83** 051117